Ultracold Fermi gas in a single-mode cavity: Cavity-mediated interaction and BCS-BEC evolution

Xiaoyong Guo,[1,*] Zhongzhou Ren,[1,2,†] Guangjie Guo,[1] and Jie Peng[1]
[1]*Department of Physics, Nanjing University, Nanjing 210093, China*
[2]*Center of Theoretical Nuclear Physics, National Laboratory of Heavy-Ion Accelerator, Lanzhou 730000, China*
(Received 17 April 2012; revised manuscript received 11 October 2012; published 7 November 2012)

We propose that the evolution of superfluidity from the Bardeen-Cooper-Schrieffer (BCS) regime to the Bose-Einstein condensation (BEC) regime can be realized using ultracold Fermi gas coupled to a single-mode cavity. By the functional integral formalism, we derive an effective atom-only action, which mimics the two-component Fermi gas with tunable two-body interaction. First, we address the features of the cavity-mediated interaction. We find that the matter-light coupling creates an effective s-wave scattering whose sign and amplitude are controlled by parameters of the cavity. Second, we discuss the fermionic superfluidity on the mean-field level, including the order parameter, chemical potential, quasiparticle excitation spectrum, momentum distribution, and dissociation temperature. It is shown that by varying the atom-cavity detuning, a BCS to BEC crossover occurs. In addition, the influences of the atomic collaborative effect and external pumping field on the pairing correlation are also studied.

DOI: 10.1103/PhysRevA.86.053605 PACS number(s): 03.75.Ss, 67.85.Lm, 03.75.Hh, 42.50.Pq

I. INTRODUCTION

Ultracold quantum gases are dilute atomic systems trapped by magnetic or optic fields and cooled to temperatures of a few tens of nano-Kelvins [1,2]. Due to their superb tunability and purity, atomic gases become ideal platforms when we put our fundamental models to the test. A particularly interesting system of such kind is the superfluid Fermi gas with a Bardeen-Cooper-Schrieffer (BCS) to Bose-Einstein condensation (BEC) evolution. The possibility to control the scattering length and thereby tune the effective attraction through the technique of Feshbach resonance [3] paves the way to investigate fermionic superfluidity as a function of interaction parameter. With the increase of the inverse s-wave scattering length from negative to positive, the fermionic superfluidity evolves from a weak-coupling BCS type to a molecular BEC type. Although the scattering length is divergent at the resonance, the evolution is not a phase transition but a smooth crossover. The original Hamiltonian with a tunable attractive interaction was first considered by Leggett [4] and more quantitative studies were then performed by Nozières and Schmitt-Rink (NSR) [5], and also by Sá de Melo [6]. Recent theoretical works that deal with more complicated cases have addressed the BCS-BEC evolution in systems as diverse as the anisotropic Fermi superfluid [7–9], relativistic Fermi and Bose-Fermi mixtures [10,11], Fermi gases with population and mass imbalance [12–14], disordered Fermi gases [15,16], and spin-orbit coupled Fermi gases [17,18]. The new findings are interesting and exciting. For instance, in the p-wave scattering case the BCS-BEC evolution turns into a quantum phase transition [7], and a topological phase transition arises when the spin-orbit coupling is taken into account [17]. Following state-of-the-art experimental techniques, some of these works have been verified in laboratories [19–21].

Besides the Feshbach resonance, there are quite different ways to introduce a tunable interaction between atoms, say by the cavity quantum electrodynamics (CQED). As an intersection of quantum optics and atomic physics, quantum gases coupled with an optical cavity have recently attracted a great deal of attention [22–24]. In this paper, we consider a system of two-level Fermi atoms strongly coupled with an optical cavity. Here the internal states of fermions are labeled as pseudospins, by analogy with the situation in superconductors. We omit the direct collision of fermions and treat them as noninteracting particles. The system also couples with the environmental degrees of freedom, which produce the pumping and dissipation channels. In recent works [25–27], a Bosonic version of this model has been investigated. It is shown that if the pump laser has sufficient intensity (typically much greater than the cavity decay rate), one instability arises: the atoms crystallize at either the even or odd antinodes of the cavity mode. In our study, we do not intend to address the self-organization of atoms. Instead, the pumping laser intensity is assumed to be sufficiently low to avoid the self-organization threshold. We demonstrate that the cavity field induces a pairwise interaction between fermions with opposite pseudospins. When the cavity mode is red-detuned from the atomic resonance, the cavity-mediated interaction (CMI) becomes attractive rather than repulsive, and thus triggers a pairing instability. We treat the atom-cavity coupling strength and the cavity decay rate as free parameters. Then, varying the atom-cavity detuning drives the superfluidity of the pairing field from the BEC type to the BCS type. In experiments, such a tunable detuning can be realized by using a two-mirror optomechanical cavity with one fixed and one movable end mirror. The position of the movable end mirror determines the photon frequencies, which directly affect the atom-cavity detuning [28–30]. In the subsequent section, we introduce the model Hamiltonian and implement the path integral approach to derive an effective action for atoms. In Sec. III, a mean-field description is developed. We solve the model at zero temperature discussing the ground-state properties. The chemical potential, order parameter, excitation spectrum, and momentum distribution are presented at this stage. Then the model is solved for the pair-breaking energy scales. We

*xiaoyongguoauthor@yahoo.cn
†zren@nju.edu.cn

also compare our results with that obtained from microcavity polaritons. Finally, a summary is given in Sec. IV.

II. MODEL

Let us consider an ensemble of two-level fermions coupled to a single-mode optical cavity. The cavity is transversely pumped by two counterpropagating laser fields of intensity Ω (Rabi frequency). These lasers create a one-dimensional optical lattice, and confine the atoms in a single antinode of this lattice to form a pancakelike cloud. For a very narrow pancake thickness, atoms would feel a constant pumping intensity. The cavity also couples to an environmental reservoir with a rate of γ, which provides a dissipation channel for the intracavity photons. The physical realization of our model is schematically depicted in Fig. 1. In the absence of the Feshbach resonance, the fermions are not allowed to have s-wave scattering by the Pauli principle. Hence, we omit the contact collision between atoms. In a frame rotating at the pumping laser frequency ω_L, the physics of the system is governed by the Hamiltonian ($\hbar = k_B = 1$)

$$\begin{aligned} H = & \int d\mathbf{r}\Big[\psi_\downarrow^\dagger(\mathbf{r})\left(-\frac{\nabla^2}{2m}-\mu\right)\psi_\downarrow(\mathbf{r})+\psi_\uparrow^\dagger(\mathbf{r}) \\ & \times\left(-\frac{\nabla^2}{2m}-\mu+\Delta_A\right)\psi_\uparrow(\mathbf{r})\Big] \\ & +\Delta_c a^\dagger a + i\int d\mathbf{r}[\psi_\uparrow^\dagger(\mathbf{r})\psi_\downarrow(\mathbf{r})(g(\mathbf{r})a+\Omega)-\text{H.c.}] \\ & +\sum_\epsilon \Delta_\epsilon A_\epsilon^\dagger A_\epsilon + \gamma\sum_\epsilon (a^\dagger A_\epsilon + A_\epsilon^\dagger a). \end{aligned} \tag{1}$$

Here, $\psi_{\uparrow,\downarrow}(\mathbf{r})$ is the annihilation operator of fermions with pseudospins $\uparrow$ or $\downarrow$ which denote the internal energy levels separated by transition frequency $\Delta_A = \omega_A - \omega_L$; μ is the chemical potential of fermions; a is the annihilation operator of cavity photons with resonant frequency $\Delta_c = \omega_c - \omega_L$; $g(\mathbf{r}) = g\,\Xi(\mathbf{r})$, where g is the atom-photon coupling constant and $\Xi(\mathbf{r})$ is the mode function of the cavity field; and A_ϵ is the annihilation operator of ϵ mode of the environmental reservoir. In Eq. (1), we have made the rotating wave approximation (RWA) to drop the energy and momentum nonconserving terms, which correspond to the virtual particle excitations.

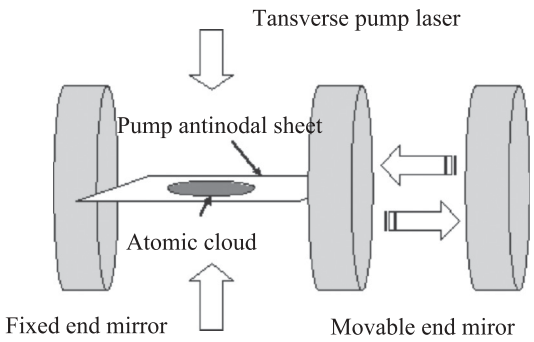

FIG. 1. Schematic diagram of the experimental realization of our model. The optomechanical cavity with one fixed and one movable end mirror is transversely pumped by two counterpropagating lasers, which create a one-dimensional optical lattice. Atoms are confined at the antinode of this lattice, and form a pancakelike cloud.

In the weak coupling regime and for a large detuning Δ_c, a cancellation effect emerges from rapid oscillation of the counterrotating terms with frequency $\Delta_A + \Delta_c$. Therefore, the RWA is implemented to disregard these terms. Physically, the RWA implies that the virtually excited particle is formed locally and decays almost instantaneously [31]. If the atoms are localized in particular sites, the Hamiltonian (1) will become the well known Dicke model, a basic model in quantum optics [32]. Then we assume that the atomic levels are sufficiently long lived. In this scenario, the pumping field can balance the cavity loss as well as the population between the two levels so as to realizing a pseudospin half system. Certainly, there are also other ways to make such an assumption valid (e.g., by coupling the two hyperfine states via the Raman transition). As a result, one could adopt a quasiequilibrium description to the thermodynamics of the system. Expressed in the coherent state path integral, the quantum partition function takes the form

$$Z = \int D(\overline{\psi}_{\uparrow\downarrow},\psi_{\uparrow\downarrow})D(a^*,a)D(A_\epsilon^*,A_\epsilon)e^{-S_{\text{at}}-S_{\text{em}}-S_{\text{int}}-S_{\text{dis}}}, \tag{2}$$

with actions

$$\begin{aligned} S_{\text{at}} = & \int d\mathbf{r}d\tau\Big[\overline{\psi}_\downarrow(\mathbf{r},\tau)\left(\partial_\tau-\frac{\nabla^2}{2m}-\mu\right)\psi_\downarrow(\mathbf{r},\tau) \\ & +\overline{\psi}_\uparrow(\mathbf{r},\tau)\left(\partial_\tau-\frac{\nabla^2}{2m}-\mu+\Delta_a\right)\psi_\uparrow(\mathbf{r},\tau)\Big], \end{aligned} \tag{3}$$

$$S_{\text{em}} = \int d\tau a^*(\tau)(\partial_\tau+\Delta_c)a(\tau), \tag{4}$$

$$S_{\text{int}} = i\int d\mathbf{r}d\tau[\overline{\psi}_\uparrow(\mathbf{r},\tau)\psi_\downarrow(\mathbf{r},\tau)(g(\mathbf{r})a(\tau)+\Omega)-\text{H.c.}], \tag{5}$$

$$\begin{aligned} S_{\text{dis}} = & \int d\tau\Big\{\sum_\epsilon A_\epsilon^*(\tau)(\partial_\tau+\Delta_\epsilon)A_\epsilon(\tau) \\ & +\gamma\sum_\epsilon[a^*(\tau)A_\epsilon(\tau)+A_\epsilon^*(\tau)a(\tau)]\Big\}, \end{aligned} \tag{6}$$

where $\tau = it$ is the imaginary time.

To proceed, we develop an effective atom-only action by integrating out the photon fields. These integrations are exactly performed since the action is entirely linear or quadratic in a as well as in A_ϵ [33]. We first carry out the Gaussian path integral over environmental degrees of freedom. Each such integration adds a term to the effective action, and their overall contribution is as follows [31,34]:

$$\int D(A_\epsilon^*,A_\epsilon)e^{-S_{\text{dis}}} = e^{-S_{\text{cl}}}, \tag{7}$$

with

$$S_{\text{cl}} = -\gamma^2\int d\tau d\tau'\sum_\epsilon n_B(\Delta_\epsilon)e^{-\Delta_\epsilon(\tau-\tau')}a^*(\tau)a(\tau'), \tag{8}$$

where $n_B(\Delta_\epsilon)$ is the Bose number. In the regime where the dissipative dynamics dominates the dispersive one, Eq. (8) might modify the physics in interesting ways. However, in the present case, the dissipation is dominated by the energy of the photons ($\sim \Delta_c$) and thereby Eq. (8) can be cast into a more

simpler form via the notion of the Markovian approximation [35]. In Eq. (8), the system-environment correlation function is read as $G(\tau-\tau')=\gamma^2\sum_\epsilon n_B(\Delta_\epsilon)e^{-\Delta_\epsilon(\tau-\tau')}$. Because the spectrum of environment is flat as in usual CQED architectures, the memory effect of the reservoir should be neglected by assuming that $G(\tau-\tau')\simeq i\kappa\delta(\tau-\tau')$, where κ is a phenomenological cavity decay rate and is a basic parameter of the cavity. With the virtue of this assumption, Eq. (8) yields

$$S_{\rm cl}=-i\kappa\int d\tau a^*(\tau)a(\tau). \tag{9}$$

Combining Eqs. (4) and (9), the action that depends on (a,a^*) can be written as

$$S'_{\rm em}=\int d\tau a^*(\tau)(\partial_\tau+\Delta_c-i\kappa)a(\tau)+S_{\rm int}. \tag{10}$$

Next, we carry out the functional integral (also Gaussian) over (a,a^*), thus arriving at an action entirely in terms of the atomic degrees of freedom. Such an atom-only action has the form

$$\begin{aligned}S'_{\rm at}=&\int d\mathbf{r}d\tau\left[\overline{\psi}_\downarrow(\mathbf{r},\tau)\left(\partial_\tau-\frac{\nabla^2}{2m}-\mu\right)\psi_\downarrow(\mathbf{r},\tau)+\overline{\psi}_\uparrow(\mathbf{r},\tau)\left(\partial_\tau-\frac{\nabla^2}{2m}-\mu+\Delta_a\right)\psi_\uparrow(\mathbf{r},\tau)\right]\\&-\frac{1}{\beta}\int d\mathbf{r}d\tau d\mathbf{r}'d\tau'\sum_n\frac{e^{i\omega_n(\tau-\tau')}}{-i\omega_n+\Delta_c-i\kappa}\Xi^*(\mathbf{r})\Xi(\mathbf{r}')\overline{\psi}_\downarrow(\mathbf{r},\tau)\psi_\uparrow(\mathbf{r},\tau)\overline{\psi}_\uparrow(\mathbf{r}',\tau')\psi_\downarrow(\mathbf{r}',\tau')\\&+i\int d\mathbf{r}d\tau[\overline{\psi}_\uparrow(\mathbf{r},\tau)\psi_\downarrow(\mathbf{r},\tau)\Omega-\Omega^*\overline{\psi}_\downarrow(\mathbf{r},\tau)\psi_\uparrow(\mathbf{r},\tau)].\end{aligned} \tag{11}$$

Within the RWA, terms that conserve the total momenta have the major contribution to the partition function. To take only these terms into account, it is convenient to transform the quartic interaction in Eq. (11) from the coordinate space to the momentum space. A straightforward Fourier transformation gives

$$\frac{1}{V}\sum_{\{\vec{k}_i\}}\int d\tau d\tau'\sum_n\frac{e^{i\omega_n(\tau-\tau')}}{-i\omega_n+\Delta_c-i\kappa}|\Xi_{\vec{l}}|^2\bar{\psi}_{\downarrow,\vec{k}_1}(\tau)\psi_{\uparrow,\vec{k}_2}(\tau)\bar{\psi}_{\uparrow,\vec{k}_3}(\tau')\psi_{\downarrow,\vec{k}_4}(\tau')\delta(\vec{l}+\vec{k}_1-\vec{k}_2)\delta(\vec{l}-\vec{k}_3-\vec{k}_4), \tag{12}$$

where vectors $\{\vec{k}_i\}(i=1,\ldots,4)$ represent momenta of fermions, and $\vec{l}$ is the wave vector of the single-mode cavity field. With the condition of the momentum conservation (i.e., $\vec{k}_2+\vec{k}_4=\vec{k}_1+\vec{k}_3$), we can denote $\vec{k}_1=\vec{p}-\vec{l}$, $\vec{k}_2=\vec{p}$, $\vec{k}_3=\vec{p}'+\vec{l}$, and $\vec{k}_4=\vec{p}'$, then perform the summation over $\{\vec{k}_3,\vec{k}_4\}$ yielding

$$\frac{1}{V}\sum_{\vec{p},\vec{p}'}\int d\tau d\tau'\sum_n\frac{e^{i\omega_n(\tau-\tau')}}{-i\omega_n+\Delta_c-i\kappa}|\Xi_l|^2\bar{\psi}_{\downarrow,\vec{p}-\vec{l}}(\tau)\psi_{\uparrow,\vec{p}}(\tau)\bar{\psi}_{\uparrow,\vec{p}'+\vec{l}}(\tau')\psi_{\downarrow,\vec{p}'}(\tau'). \tag{13}$$

Notice that the effective atom-atom interaction now becomes local in space. Moreover, for the detuning $|\Delta_c|$ larger than the other relevant energy scales, the summation over ω_n is approximated as $\frac{\Delta_c\beta}{\Delta_c^2+\kappa^2}\delta(\tau-\tau')$. Gathering these results and backing to the coordinate space, Eq. (11) reduces to the following simpler form:

$$\begin{aligned}S'_{\rm at}=&\int d\mathbf{r}d\tau\left[\overline{\psi}_\downarrow(\mathbf{r},\tau)\left(\partial_\tau-\frac{\nabla^2}{2m}-\mu\right)\psi_\downarrow(\mathbf{r},\tau)+\overline{\psi}_\uparrow(\mathbf{r},\tau)\left(\partial_\tau-\frac{\nabla^2}{2m}-\mu+\Delta_a\right)\psi_\uparrow(\mathbf{r},\tau)\right]\\&+\frac{g^2\Delta_c}{\Delta_c^2+\kappa^2}\int d\mathbf{r}d\tau|\Xi|^2\overline{\psi}_\downarrow(\mathbf{r},\tau)\overline{\psi}_\uparrow(\mathbf{r},\tau)\psi_\uparrow(\mathbf{r},\tau)\psi_\downarrow(\mathbf{r},\tau)\\&+i\int d\mathbf{r}d\tau[\overline{\psi}_\uparrow(\mathbf{r},\tau)\psi_\downarrow(\mathbf{r},\tau)\Omega-\Omega^*\overline{\psi}_\downarrow(\mathbf{r},\tau)\psi_\uparrow(\mathbf{r},\tau)].\end{aligned} \tag{14}$$

In the above equation, the CMI has a form of the s-wave scattering, whose magnitude and sign can be manipulated by the physical parameters of cavity. We also note that for $\Delta_c>0$ the interaction is repulsive. In this case, the system is trivial since the effect of CMI is nothing but collision. With such repulsion the atoms cannot bond with each other into pairs. However, if the cavity resonant frequency is red-detuned from the pumping laser (i.e., $\Delta_c<0$) the pairwise interaction becomes attractive rather than repulsive. In this circumstances, the action (14) mimics the action of two-component Fermi gas with the Feshbach resonance. Therefore it is quite natural to surmise that a pairing instability will show up and the superfluidity of these pairs will evolve with the intensity of the attraction. We leave this important issue momentarily and discuss it later with the solutions of the mean-field equation.

Introducing the usual Hubbard-Stratonovich field $\phi(\mathbf{r},\tau)$, which couples to $\bar{\psi}_\uparrow\bar{\psi}_\downarrow$, and under the Nambu spinor basis

$\Psi = (\psi_\uparrow, \psi_\downarrow, \bar{\psi}_\downarrow, \bar{\psi}_\uparrow)^T$, Eq. (14) yields

$$S_{\text{eff}} = \int d\mathbf{r}d\tau \frac{\Delta_c^2 + \kappa^2}{g^2\Delta_c}|\phi|^2 - \int d\mathbf{r}d\tau \bar{\Psi}\hat{G}^{-1}\Psi, \quad (15)$$

where

$$\hat{G}^{-1} = \begin{pmatrix} -\partial_\tau + \frac{\nabla^2}{2m} + \mu + \Omega\sigma_y & -\phi\Xi\sigma_z \\ \bar{\phi}\Xi^*\sigma_z & -\partial_\tau - \frac{\nabla^2}{2m} - \mu - \Omega\sigma_y \end{pmatrix} \quad (16)$$

is the inverse Nambu propagator. Here, σ_y and σ_z are the Pauli matrices. After integrating out the fermions $(\Psi, \bar{\Psi})$, we obtain an action for pairing field alone, that is,

$$S'_{\text{eff}} = \int d\mathbf{r}d\tau \frac{\Delta^2 + \kappa^2}{g^2\Delta}|\phi|^2 - \text{tr}\ln\hat{G}^{-1}. \quad (17)$$

In Eqs. (16) and (17), the external laser field has been tuned on resonance with the atomic transition, $\omega_A = \omega_L$, and $\Delta = \omega_c - \omega_A$ represents the atom-cavity detuning. So far, Eqs. (14) and (17) are the main results of our functional integral treatment. In the following section, we subject the action (17) to a saddle-point analysis. This will address the possibility of observing the superfluidity of the fermion pairs and the BCS-BEC evolution when the parameters of cavity are varied.

III. MEAN-FIELD DESCRIPTION

In this section, we develop a mean-field description to investigate the superfluidity of pairs forged by the CMI. When we replace the field $\phi(\mathbf{r},\tau)$ by its static and homogeneous counterpart ϕ_0, a saddle-point action, $S'_{\text{eff}}(\phi_0)$, is attained. We then proceed by minimizing the saddle-point action to obtain the order parameter equation. For the action (17), the saddle-point equation assumes the form

$$\frac{\delta S'_{\text{eff}}}{\delta\bar{\phi}_0} = \frac{\Delta^2 + \kappa^2}{g^2|\Delta|}\phi_0 - \text{tr}\hat{G}\frac{\delta\hat{G}^{-1}}{\delta\bar{\phi}_0} = 0. \quad (18)$$

A straightforward calculation of the trace term in Eq. (18) provides that

$$\text{tr}\hat{G}\frac{\delta\hat{G}^{-1}}{\delta\bar{\phi}_0} = -T\sum_{n,p}\frac{4\phi_0|\Xi|^2\left(\omega_n^2 + \xi_p^2 + |\phi_0\Xi|^2 - |\Omega|^2\right)}{\det\hat{G}_{n,p}^{-1}}, \quad (19)$$

with

$$\begin{aligned}\det\hat{G}_{n,p}^{-1} = {} & (i\omega_n)^4 - 2\left(\xi_p^2 + |\Omega|^2 + |\phi_0\Xi|^2\right)(i\omega_n)^2 \\ & + \left(\xi_p^4 - 2|\Omega|^2\xi_p^2 + 2|\phi_0\Xi|^2\xi_p^2\right. \\ & \left. + |\Omega|^4 - 2|\phi_0\Xi|^2|\Omega|^2 + |\phi_0\Xi|^4\right). \end{aligned} \quad (20)$$

In Eqs. (19) and (20), we have transformed to a frequency-momentum space where $\omega_n = (2n+1)\pi T$ stands for the fermionic Matsubara frequency and $\xi_p = p^2/2m - \mu$ is the kinetic energy minus the chemical potential. The singularities of $\hat{G}_{n,p}$ can be worked out explicitly. These singularities represent the quasiparticle excitation energy, $E_p = \pm(\sqrt{\xi_p^2 + |\phi_0\Xi|^2} \pm |\Omega|)$, where the factors $\pm$ in front of the bracket correspond to the particle and hole branches. After straightforwardly calculating the Matsubara summation, we arrive at an order parameter equation of familiar form

$$\frac{\Delta^2 + \kappa^2}{g^2|\Delta|} = |\Xi|^2\sum_p \frac{1}{2E_p^0}[1 - f(E_p^+) + f(E_p^-)], \quad (21)$$

where $E_p^0 = \sqrt{\xi_p^2 + |\phi_0\Xi|^2}$, $f(z) = 1/(\exp(\beta z) + 1)$ is the Fermi function, and $E_p^\pm = \sqrt{\xi_p^2 + |\phi_0\Xi|^2} \pm |\Omega|$ are the particle branches of E_p. For a single-mode cavity, the intensity distribution in frequency space can be written as $|\Xi|^2 = \kappa^2/(\kappa^2 + \Delta^2)$, which is broadened by κ^2 and peaked at around $\Delta = 0$. Save for Eq. (21), an additional equation relating the fermion number to the temperature and chemical potential is required. Taking the derivative of the saddle-point action $S'_{\text{eff}}(\phi_0)$ with respect to μ, and using $n = -T\partial S'_{\text{eff}}(\phi_0)/\partial\mu$, we have

$$n = \sum_p \left\{1 - \frac{\xi_p}{E_p^0}[1 - f(E_p^+) + f(E_p^-)]\right\}. \quad (22)$$

In the following two subsections, we explore the impact of the CMI on the unitary Fermi gas by solving Eqs. (21) and (22).

A. Zero-temperature solution

At zero temperature there are four parameters remaining: the dimensionless atom-cavity detuning $|\Delta|/\kappa$, the collaborative factor $\zeta = ng^2/\kappa^2$, the pumping field Rabi frequency $|\Omega|/\kappa$, and the relative energy scale $\Lambda = \varepsilon_F/\kappa$. Here, $\varepsilon_F = p_F^2/2m$ is the Fermi energy with the Fermi momentum p_F. We also note that for $\beta \to \infty$, the terms dependent on the pumping field intensity $|\Omega|$ disappear in both the order parameter and number equations. As a result, the pair-breaking effect of the pumping laser has no influence on the zero-temperature properties of the condensate. The scales of parameters used for the numerical solutions of Eqs. (21) and (22) can be obtained from the following considerations. For an experimentally realizable optomechanical cavity with one movable end mirror, the cavity decay rate is comparable with coupling constant, $\kappa \simeq g$, and both may have the order of $10^6\ \text{s}^{-1}$ [36]. For an ensemble of ^{6}Li atoms, a typical value of the Fermi energy may be $\varepsilon_F = 4.9 \times 10^{-29}$ J that is quoted directly from Zwierlein *et al.* [37]. Thereby, for the Planck constant $h = 6.626 \times 10^{-34}\ \text{J} \times s$, the relative energy scale will have the order of $\Lambda \sim 10^{-1}$. In the following we will show that to obtain the superfluidity, values of detuning $|\Delta|/\kappa$ should belong to the interval $(10, 100)$, and in which the condition $|\Delta| \gg \kappa$ is well satisfied. We plot the reduced order parameter $|\phi_0|/\varepsilon_F$ and the dimensionless chemical potential μ/ε_F (inset) as a function of the detuning $|\Delta|/\kappa$, for $\zeta = 10^3$ in Fig. 2(a) and $\zeta = 10^4$ in Fig.2(b). The relative energy scale is fixed to be $\Lambda = 0.1$ throughout the paper. In the studies of ultracold Fermi gases with the Feshbach resonance, a scattering parameter (scattering length) is introduced to regulate the ultraviolet divergence in the saddle-point equation. However for the present case where the coupling strength does not play the role of control parameter, one needs to truncate the momentum integral at a finite value to avoid the ultraviolet divergence [10]. To fully taken into account the low temperature and long wave length properties, the cutoff

momentum p_c is chosen to be of the order of $100p_F$ in Eqs. (21) and (22).

In Fig. 2(a) it is shown that $|\phi_0|$ first increases and then decreases to zero with increasing $|\Delta|$. The maximum value of $|\phi_0|$ is reached at around $|\Delta|/\kappa = 20$ (solid line). This nonmonotonous behavior reflects a complicated dependence of order parameter on the atom-cavity detuning. The existence of nonvanishing order parameter means that the fermion pairs created by CMI are condensed into a coherent state (i.e., fermionic superfluid). We also note that as $|\Delta|$ increases, the chemical potential grows and smoothly evolves from negative to positive. This is the signature of the evolution between BEC- and BCS-type superfluid. Moreover, when $|\Delta|/\kappa > 40$ (solid line), the order parameter vanishes and the chemical potential tends to ε_F. Therefore, we identify the small detuning regime ($|\Delta|/\kappa < 30$) as the strong-coupling BEC limit and the large detuning regime ($|\Delta|/\kappa > 40$) as the opposite weak-coupling BCS limit. The dependence of our numerical results on cutoff momentum p_c is also demonstrated in Fig. 2. We note that values of p_c do not affect the system in any qualitative way. Therefore we shall use $p_c = 100p_F$ in the following discussions. Before going on, the two limiting cases can be addressed analytically. As anticipated, the number equation fixes the chemical potential, $\mu = \varepsilon_F$, at the weak coupling limit. Then the solution of saddle-point equation is $\phi_0/\varepsilon_F \sim (\Delta/\kappa)\exp(-\frac{\kappa}{g^2\nu}(\frac{\Delta}{\kappa})^3)$, where $\varepsilon = p^2/2m$ is the kinetic energy and we have assumed that the density of states $\nu(\varepsilon)$ is roughly constant $\nu = \nu(\varepsilon_F)$. In the strong coupling limit, we use $\mu < 0$ to solve Eq. (22) yielding the result $|\phi_0\Xi| \sim \sqrt{(\varepsilon_c + 2|\mu|)^2 - (\varepsilon_c - n/\nu\varepsilon_F)^2}$, where ε_c is the cutoff energy for the integral in Eq. (22). Limiting analytical expressions tell us that in the BCS limit, the order parameter vanishes nearly exponentially with the increase of detuning, while it remains a finite value proportional to $|\mu|$ in the opposite BEC limit. As a matter of fact, these features are just what we read from Fig. 2.

To understand the underlying physics of these results, one needs to recall that the cavity photon plays the role of medium to generate and propagate the effective interaction for atoms. The picture is similar to the usual BCS superconductors where the electron-phonon scattering creates the attractive interaction. A large atom-cavity detuning has a detrimental effect on the process of atoms emitting photons into the cavity mode, same as in CMI. For the cavity mode nearly resonant with the atomic transition, CMI is strong enough to forge diatomic molecular. When the opposite is true, the weak attraction will bound atoms into Cooper pairs. With the further increasing of detuning, the pairs disassociate into atoms. Beyond a certain detuning (say, 40κ), the superfluid ordering is likely to be lost and we have a free Fermi gas which is characterized by $\mu = \varepsilon_F$. The amplitude of the order parameter and the domain of superfluidity are all enlarged by a greater collaborative factor, $\zeta = 10^4$, as shown in Fig. 2(b). Notice that the BEC region is also bigger than the previous case, and the BCS to BEC evolution takes place at around $|\Delta|/\kappa \approx 70$ (solid line). These consequences are somewhat expected because CMI has been enhanced by a large matter-light coupling along with a small cavity decay rate. Therefore, the pair-breaking effect of detuning can be suppressed by the collaborative effect.

At zero temperature, the pumping field intensity $|\Omega|$ is irrelevant. The particle branch of the excitation spectrum, E_p^0, and the momentum distribution, $n_p = [1 - \frac{\xi_p}{E_p^0}]/2$, have important roles in the thermodynamic properties of the BCS-BEC evolution. In Fig. 3, we demonstrate E_p^0/ε_F and n_p as a function of $|p| = \sqrt{p_x^2 + p_y^2}$ (in units of p_F) for both $\zeta = 10^3$ and $\zeta = 10^4$ cases. Here, the cutoff momentum is $p_c = 100p_F$ and the BEC side is shown as dashed line for $|\Delta|/\kappa = 10$, whereas the solid line represents the BCS side for $|\Delta|/\kappa = 10^2$. We find a nonanalytic behavior of E_p^0 when $\mu = 0$. There is a gapless spectrum in the BCS region and a fully gapped spectrum in the opposite BEC region (see the upper left in Fig. 3). The quasiparticle excitation

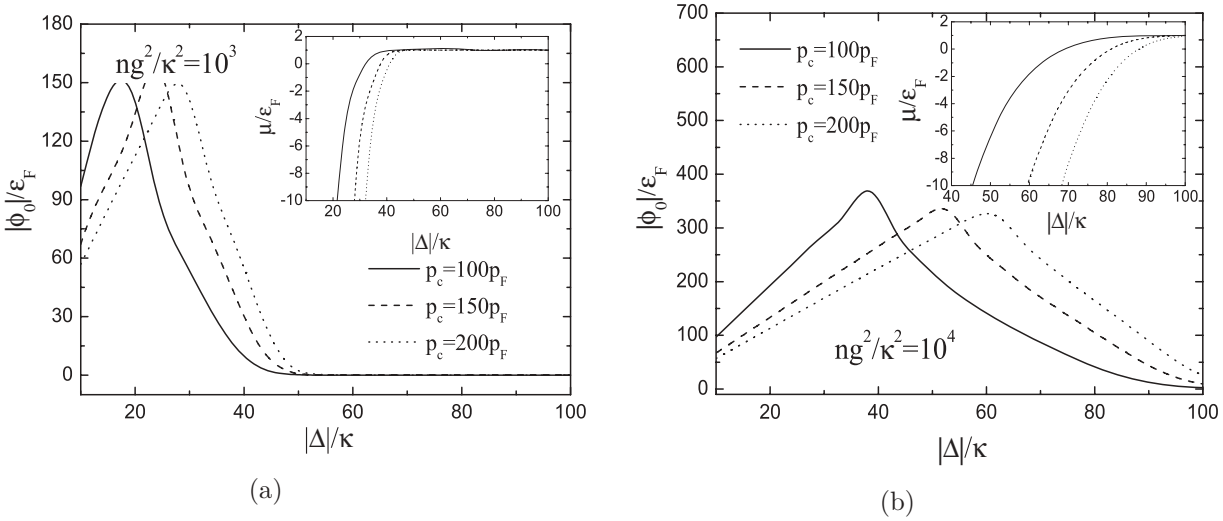

FIG. 2. The reduced order parameter $|\phi_0|/\varepsilon_F$ and dimensionless chemical potential μ/ε_F (inset) as a function of the detuning $|\Delta|/\kappa$ at zero temperature, for (a) $\zeta = 10^3$ and (b) $\zeta = 10^4$. Here, the relative energy scale is given to be $\Lambda = 0.1$, and the cutoff momentum p_c is taken as $p_c = 100p_F$ (solid line), $p_c = 150p_F$ (dashed line), and $p_c = 200p_F$ (dotted line).

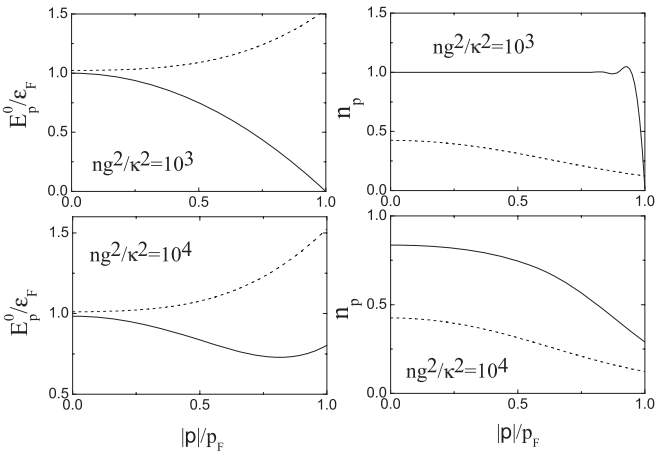

FIG. 3. Plots for E_p^0/ε_F and n_p as a function of $|p| = \sqrt{p_x^2 + p_y^2}$ (in units of p_F) at zero temperature, for $\zeta = 10^3$ in the top row and $\zeta = 10^4$ in the bottom row. Here, the BEC case is shown as a dashed line for $|\Delta|/\kappa = 10$, while the solid line represents the BCS case for $|\Delta|/\kappa = 10^2$. The relative energy scale is given to be $\Lambda = 0.1$, and the cutoff momentum is $p_c = 100 p_F$.

spectrum is gapless unless the conditions $\phi_0 = 0$ and $\mu = \varepsilon_F$ are both satisfied [38]. To fulfill the second condition, the system has to reside in the BCS regime where $\mu > 0$, and therefore the spectrum is always gapped in the BEC side. For the nonzero angular momentum superfluid (say, p-wave superfluid), the quasiparticle excitation spectrum may be gapless in the BCS side since the order parameter is angular dependent, which possesses zero points in momentum space [8]. However, the order parameter is isotropic in our model, thus a gapless spectrum in the BCS side means the vanishing of pairing field rather than encountering a zero point. Hence, the BCS-BEC evolution in our model is not a phase transition but a crossover. This statement shall be seen clearly in the momentum distribution. A comparison between the BEC and BCS cases in the second column of Fig. 3 shows that as the detuning decreases the Fermi distribution with locus $\xi_p = 0$ is deformed, and n_p broadens in the BEC side. We can infer that since the CMI is enhanced by the small detuning, two atoms with opposite momenta become more tightly bound. As a result, the fermions with larger momentum will likely participate in the formation of bound states. Without any qualitative changes in momentum distribution, we conclude that the evolution is a crossover. From the bottom row of Fig. 3, it turns out that a stronger collaborative effect has no influence on the BEC side. Nevertheless, as we already mentioned, it is helpful in the formation of bound pairs. Consequently, the departure of n_p from the Fermi distribution becomes more obvious and fully gapped quasiparticle spectrums in both sides are obtained. The conclusions we read from Fig. 3 are in agreement with those in Fig. 2.

B. Disassociation temperature

We are now in a position to explore the pair-breaking temperature scale, $T_{\rm dis}$, defined as the temperature at which some fixed fraction of the bound pairs are dissociated. To this end, Eqs. (21) and (22) are solved with vanishing order parameter $|\phi_0| = 0$. Different from the previous case, the pumping field intensity $|\Omega|$ is involved in the calculations. Similar with the usual BCS theory, we get that $T_{\rm dis}/\varepsilon_F \sim \exp(-\frac{\kappa}{g^2\nu}(\frac{\Delta}{\kappa})^3)$ (i.e., $T_{\rm dis}$ decreases exponentially in the BCS limit). Nevertheless, in the BEC regime with a negative chemical potential $\mu < 0$, the number equation yields that $\cosh(\frac{|\mu|}{2T_{\rm dis}})\exp(\frac{n}{2\nu T_{\rm dis}}) = \cosh(\frac{\varepsilon_c+|\mu|}{2T_{\rm dis}})$. Because $\frac{|\mu|}{2T_{\rm dis}} \gg \frac{\varepsilon_c}{2T_{\rm dis}}$ in the BEC limit, the hyperbolic functions can be divided out from both sides of the above equation. This provides that $\exp(\frac{n}{2\nu T_{\rm dis}}) \simeq 1$. To satisfy such a limiting condition, a temperature scale of $T_{\rm dis}$ without upper boundary is required. In fact, the apparent divergence of $T_{\rm dis}$ in the strong coupling limit is an artifact of the mean-field analysis. Physically, $T_{\rm dis}$ represents the dissociation energy of the pair rather than the temperature at which the coherence is established. There is a regime of temperature above the condensation temperature where the gas still remains as a strongly interacting soup with pairing correlations (often called preformed pairs in the literature [39]).

In Fig. 4, we show the direct numerical solution of $T_{\rm dis}/\varepsilon_F$ and μ_c/ε_F (inset) as a function of $|\Delta|/\kappa$ for $\zeta = 10^3$ in Fig. 4(a) and $\zeta = 10^4$ in Fig. 4(b). Here, the cutoff momentum is $p_c = 100 p_F$. The pumping field intensities are set to be $|\Omega|^2/\kappa^2 = 0.1$ (solid line) and $|\Omega|^2/\kappa^2 = 0$ (dashed line). The aim is to see how the symmetry-breaking effect of the pumping field affects the results. In Fig. 4, a monotonic dependence of $T_{\rm dis}$ on $|\Delta|/\kappa$ is revealed: with the increase of $|\Delta|/\kappa$, $T_{\rm dis}$ decreases to zero for the case of $|\Omega|^2/\kappa^2 = 0.1$ while staying at a nonvanishing value for the case of $|\Omega|^2/\kappa^2 = 0$. The disassociation temperature tends to zero meaning that all pairs disassemble to constituent fermions at the finite temperature. $T_{\rm dis}$ goes to a very high value at BEC limit owing to paring correlations above the condensation temperature. We also note that the symmetry breaking effect of the pumping field indeed suppresses the pairing correlation, but the preformed pairs are not fully destroyed since only weak pumping intensity is involved. In the inset of Fig. 4, the dependence of μ_c on Δ is qualitatively coincident with the zero-temperature solutions, and the emergence of BCS-BEC crossover is accompanied by the sharp decrease of $T_{\rm dis}$. For $\zeta = 10^4$, fermions are in favor of being associated into a bound state. Therefore, the value of $T_{\rm dis}$ is higher than the previous case, and the crossover takes place at a larger value of $|\Delta|/\kappa$.

It is clearly demonstrated that the atom-cavity detuning and the collaborative factor influence the system in different ways, and that the former plays a major role in shaping and determining the superfluidity of fermions. Our numerical calculations are supported well by the corresponding analytical considerations. In experiments, the phenomena presented above can be observed by measuring the momentum distribution [40].

C. Comparison with polariton systems

In the past, the investigations of the polariton condensation in solid as well as in microcavity systems have attracted enormous attention [41]. As a coupled matter-light system, polaritons are quasiparticles resulting from strong coupling between localized excitons (electronic excitations) and

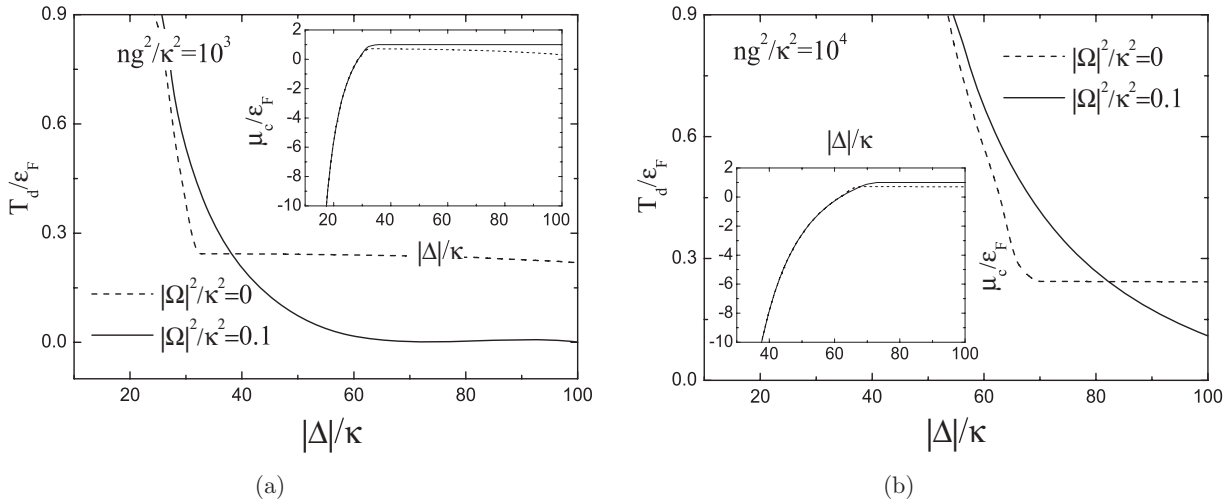

FIG. 4. The disassociation temperature $T_{\rm dis}/\varepsilon_F$ and critical chemical potential μ_c/ε_F (inset) with increasing detuning $|\Delta|/\kappa$ for (a) $\zeta = 10^3$ and (b) $\zeta = 10^4$. Here, the relative energy scale is given to be $\Lambda = 0.1$, the cutoff momentum is $p_c = 100p_F$, and the pumping field intensities are $|\Omega|^2/\kappa^2 = 0.1$ (solid line) and $|\Omega|^2/\kappa^2 = 0$ (dashed line).

photons [42]. In a recent work [43], a BCS-BEC crossover of the polariton condensate is predicted. At low excitation densities the condensation temperature T_c behaves like point bosons, while T_c approaches the BCS-like mean-field result at higher excitation densities. Notice that the mean-field equations (21) and (22), derived for an atomic system, have a common form for those two distinguishable coupled matter-light systems. Therefore, it is of interest to compare our system to the polariton one studied in [43]. The absence of a direct pairwise scattering indicates that the strength of the effective interaction is entirely due to CMI. In our model, the intensity of CMI depends on the atom-cavity detuning, and the fermion pairs are the object that undergoes the condensation and BEC-BCS crossover. The sign of chemical potential changes when the crossover takes place. For polariton condensate, however, the behavior of T_c determines which type of the superfluidity belongs. The density dependence of T_c is due to the changing coupling strength and occupation of two-level excitons with changing chemical potential. Moreover for localized excitons, the density of states is a δ function, whereas for interacting atomic gas it is nonzero for all energies greater than zero. An immediate consequence is the different interpretation of the mean-field equations. In our model, the number equation (22) alone fixes the chemical potential in the BCS side, and in the opposite BEC limit the roles of Eqs. (21) and (22) are reversed. This means that in the Fermi gases the temperature and the chemical potential are neatly separated. For localized fermions, the chemical potential lies below the band of fermions, and so the density is controlled by the tail of the Fermi distribution. As a result, the temperature and the chemical potential are not so clearly separated. In addition, for polaritons formed in zero-dimensional cavity, the mean-field theory gives the condensation temperature at both the BCS and BEC sides. For atomic systems, the mean-field approximation on the BEC side gives just the dissociation energy of molecules rather than the condensation temperature.

IV. CONCLUSION

In summary, we have investigated the system consisting of a two-component free Fermi gas coupled with a single-mode cavity. We also consider the environmental degrees of freedom, which provide the dissipation and pumping channels. We have found that when the dispersive dynamics dominates ($|\Delta_c|/\kappa \gg 1$), the matter-light coupling generates a single instability to s-wave pairing between atoms of different internal states (i.e., opposite pseudospins). The value and sign of such interaction can be controlled by the cavity geometry. Using coherent state path integral formalism, we develop a mean-field theory to describe our model, and explore the properties and impacts of the CMI. We have shown that when the cavity mode is red-detuned from the atomic resonance, the CMI becomes attractive, and thus it triggers a pairing mechanism of fermions with opposite momenta and pseudospins. In this case, intracavity photons play the role of phonons to induce the attraction as in the usual superconductors. Ground-state ($T = 0$) solution indicates that for a certain collaborative factor, the superfluidity of bounded pairs can occur. By varying the atom-cavity detuning, the superfluidity evolves between the BCS and BEC limits. The strong coupling BEC regime is found when the detuning is small. However, in the large detuning case, we obtain the weak coupling BCS regime. Although the quasiparticle excitation energy may be gapless in the BCS side while fully gapped in the BEC side, the evolution is still a smooth crossover. For the vanishing order parameter, we compute the temperature scale of pair breaking (i.e., the disassociation temperature $T_{\rm dis}$). The disassociation temperature shows a monotonically decreasing behavior with the increasing detuning, and no upper boundary found in the BEC limit means that only at very high temperatures do the molecules dissociate into atoms. The pairing correlation is suppressed by the symmetry-breaking effect of the pumping laser, but it survives in certain regimes because we only consider the weak pumping intensity $|\Omega|^2/\kappa^2 \ll 1$. Moreover, we also find that the atom-cavity detuning and the collaborative

effect play contrary roles. The former tends to break the pairs and the latter favors of tightly bounded states.

The present paper is an extension of the concept of quantum simulators by using cavity to create controllable interaction. The CMI captures the essential physics of the Feshbach resonance, making this system a promising alterative candidate for observing BEC-BCS crossover. Theoretically the physical realization of our model may work, but with state-of-the-art experimental techniques there could be some difficulties. We expect that such a proposal will be realized with the development of modern experimental techniques. The mean-field calculation in the present paper can be improved by incorporating Gaussian pair fluctuations. Moreover, it would be of considerable interest to extend our model, for example, by including the nonequilibrium pumping and dissipation. This could be done using the real time Schwinger-Keldysh functional integral formalism [44], and it is worthy to explore in the future.

ACKNOWLEDGMENTS

This work is supported by the National Natural Science Foundation of China (Grants No. 10735010, No. 10975072, No. 11035001, and No. 11120101005), by the 973 National Major State Basic Research and Development of China (Grants No. 2007CB815004 and No. 2010CB327803), by CAS Knowledge Innovation Project No. KJCX2-SW-N02, by Research Fund of Doctoral Point (RFDP), Grants No. 20100091110028, and by a Project Funded by the Priority Academic Program Development of Jiangsu Higher Education Institutions (PAPD).

[1] W. Ketterle, D. Durfee, and D. Stamper-Kurn, in *Proceedings of the International School of Physics "Enrico Fermi"*, Vol. CXL (IOS Press, Amsterdam, Oxford, Tokyo, Washington DC, 1999), p. 67.

[2] W. Ketterle and M. Zwierlein, in *Ultracold Fermi Gases*, Proceedings of the International School of Physics "Enrico Fermi," Course CLXIV, edited by M. Inguscio, W. Ketterle, and C. Salomon (IOS Press, Amsterdam, 2008); reprinted in Riv. Nuovo Cimento **31**, 247 (2008).

[3] H. Feshbach, *Theoretical Nuclear Physics* (Wiley, New York, 1992).

[4] A. J. Leggett, J. Phys. (Paris) **41**, C7 (1980).

[5] P. Nozières and S. Schmitt-Rink, J. Low Temp. Phys. **59**, 195 (1985).

[6] C. A. R. Sá de Melo, M. Randeria, and J. R. Engelbrecht, Phys. Rev. Lett. **71**, 3202 (1993).

[7] M. Iskin and C. A. R. Sá de Melo, Phys. Rev. Lett. **96**, 040402 (2006).

[8] M. Iskin and C. A. R. Sá de Melo, Phys. Rev. A **74**, 013608 (2006).

[9] M. Iskin and C. A. R. Sá de Melo, Phys. Rev. B **72**, 224513 (2005).

[10] J. Deng, A. Schmitt, and Q. Wang, Phys. Rev. D **76**, 034013 (2007).

[11] L. He and P. Zhuang, Phys. Rev. D **75**, 096003 (2007).

[12] G. B. Partridge, W. Li, R. I. Kamar, Y. Liao, and R. G. Hulet, Science **311**, 503 (2006).

[13] M. Taglieber, A. C. Voigt, T. Aoki, T. W. Hänsch, and K. Dieckmann, Phys. Rev. Lett. **100**, 010401 (2008).

[14] D. E. Sheehy and L. Radzihovsky, Ann. Phys. (N.Y.) **322**, 1790 (2007).

[15] L. Han and C. A. R. Sá de Melo, New J. Phys. **13**, 055012 (2011).

[16] G. Orso, Phys. Rev. Lett. **99**, 250402 (2007).

[17] M. Gong, S. Tewari, and C. Zhang, Phys. Rev. Lett. **107**, 195303 (2011).

[18] H. Hu, L. Jiang, X. J. Liu, and H. Pu, Phys. Rev. Lett. **107**, 195304 (2011).

[19] S. Giorgini, L. P. Pitaevskii, and S. Stringari, Rev. Mod. Phys. **80**, 1215 (2008).

[20] L. Sanchez-Palencia and M. Lewenstein, Nature Phys. **6**, 87 (2010).

[21] Y. J. Lin, K. J. García, and I. B. Spielman, Nature (London) **471**, 83 (2011).

[22] J. Larson, G. Morigi, and M. Lewenstein, Phys. Rev. A **78**, 023815 (2008).

[23] H. Zoubi and H. Ritsch, Phys. Rev. A **80**, 053608 (2009).

[24] I. B. Mekhov and H. Ritsch, J. Phys. B: At. Mol. Opt. Phys. **45**, 102001 (2012).

[25] J. K. Asboth, P. Domokos, H. Ritsch, and A. Vukics, Phys. Rev. A **72**, 053417 (2005).

[26] F. Brennecke, T. Donner, S. Ritter, T. Bourdel, M. Kohl, and T. Esslinger, Nature (London) **450**, 268 (2007).

[27] D. Nagy, G. Szirmai, and P. Domokos, Eur. Phys. J. D **48**, 127 (2008).

[28] J. D. Thompson, B. M. Zwickl, A. M. Jayich, F. Marquardt, S. M. Girvin, and J. G. E. Harris, Nature (London) **452**, 72 (2008).

[29] G. Heinrich, J. G. E. Harris, and F. Marquardt, Phys. Rev. A **81**, 011801 (2010).

[30] E. Verhagen, S. Deléglise, S. Weis, A. Schliesser, and T. J. Kippenberg, Nature (London) **482**, 63 (2012).

[31] S. Gopalakrishnan, B. L. Lev, and P. M. Goldbart, Nature Phys. **5**, 845 (2009).

[32] Xiaoyong Guo, Zhongzhou Ren, and Zimeng Chi, J. Opt. Soc. Am. B **28**, 1245 (2011).

[33] A. Altland and B. Simons, *Condensed Matter Field Theory* (Cambridge University Press, Cambridge, 2006).

[34] Xiaoyong Guo, Zhongzhou Ren, Guangjie Guo, and Bo Zhou, Can. J. Phys. **90**, 45 (2012).

[35] M. Orszag, *Quantum Optics: Including Noise Reduction, Trapped Ions, Quantum Trajectories, and Decoherence* (Springer-Verlag, Berlin, 2000).

[36] K. Baumann, C. Guerlin, F. Brennecke, and T. Esslinger, Nature (London) **464**, 1031 (2010).

[37] M. W. Zwierlein, C. A. Stan, C. H. Schunck, S. M. F. Raupach, A. J. Kerman, and W. Ketterle, Phys. Rev. Lett. **92**, 120403 (2004).

[38] Xiaoyong Guo, Zhongzhou Ren, and Zimeng Chi, Phys. Rev. A **85**, 023608 (2012).

[39] M. Randeria, Nature Phys. **6**, 561 (2010).
[40] R. Combescot, J. Low Temp. Phys. **145**, 267 (2006).
[41] H. Deng, H. Haug, and Y. Yamamoto, Rev. Mod. Phys. **82**, 1489 (2010), and references therein.
[42] C. F. Klingshirn, *Semiconductor Optics* (Springer, Berlin, 1997).
[43] J. Keeling, P. R. Eastham, M. H. Szymanska, and P. B. Littlewood, Phys. Rev. Lett. **93**, 226403 (2004); Phys. Rev. B **72**, 115320 (2005).
[44] S. Gopalakrishnan, B. L. Lev, and P. M. Goldbart, Phys. Rev. A **82**, 043612 (2010).